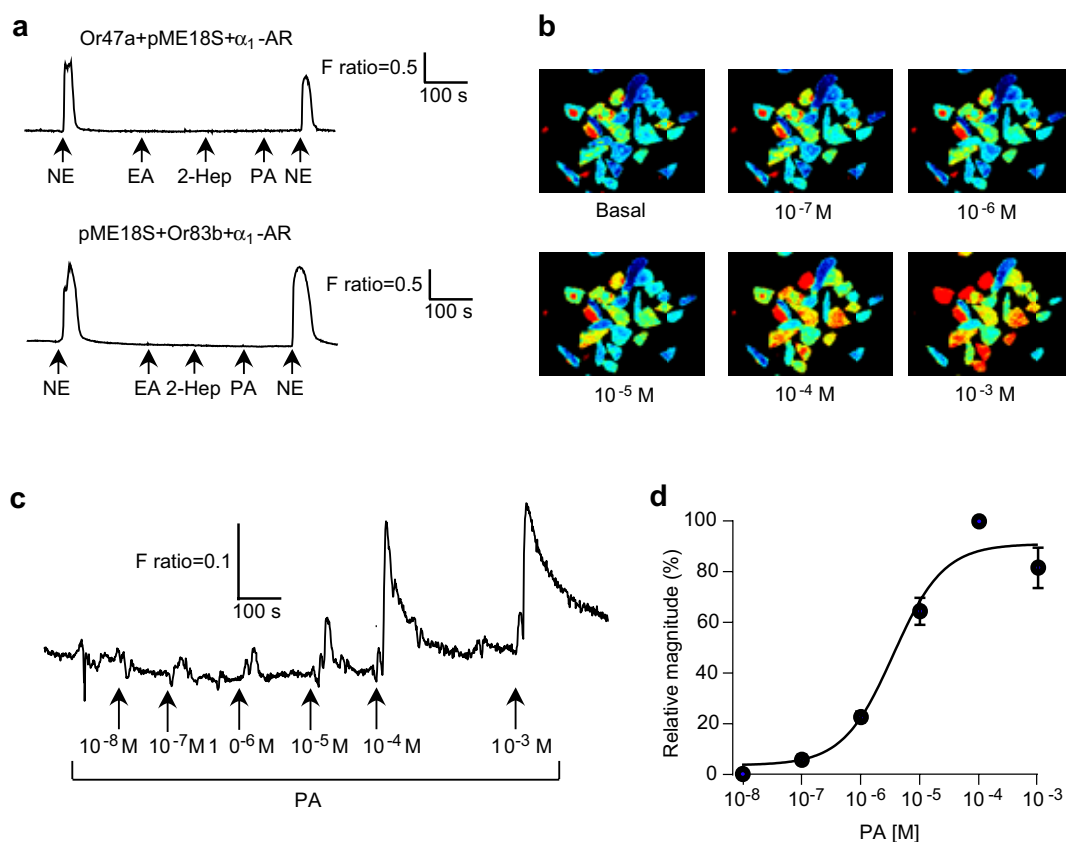
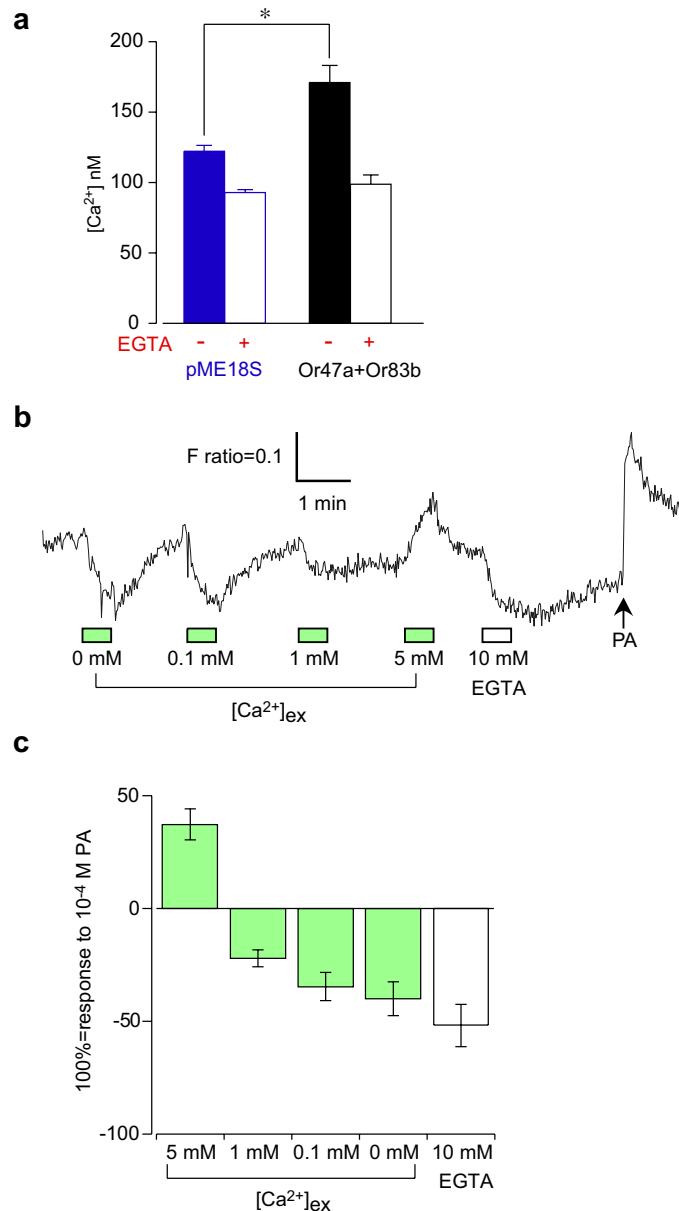


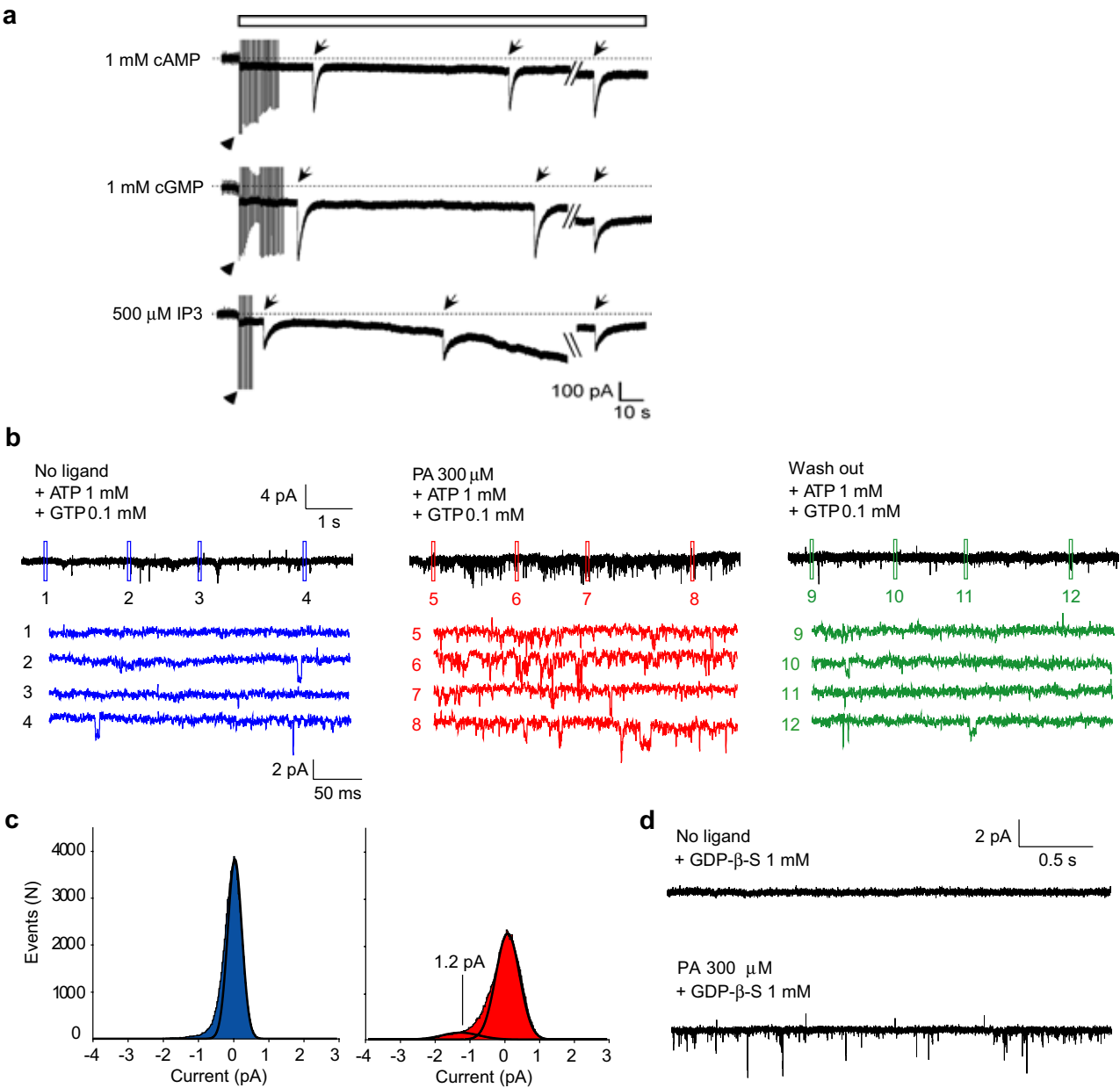
## SUPPLEMENTARY INFORMATION



**Supplementary Figure S1| Pentyl acetate-evoked  $\text{Ca}^{2+}$  responses in HeLa cells expressing Or47a+Or83b.** **a**, Fura-2-based  $\text{Ca}^{2+}$  profiles of HeLa cells transfected with Or47a and empty plasmid vector, pME18S (*upper panel*) and with pME18S and Or83b (*lower panel*). All cells were co-transfected with  $\alpha_1$ -AR as a positive control. Odorants (0.1 mM each, EA: ethyl acetate: 2-Hep: 2-heptanone; PA: pentyl acetate) and 100 nM norepinephrine (NE) were delivered to a recording chamber for 10 sec. **b-d**, Dose-dependent responses to PA of HeLa cells expressing Or47a+Or83b. **b**, Pseudocolored images of changes in Fura-2 fluorescence at various concentrations of PA where *red* corresponds to the greatest response. **c**, Fura-2-based  $\text{Ca}^{2+}$  response profiles to various concentrations of PA. **d**, Dose-response curve of Or47a+Or83b to PA. The curve was fitted to the Hill equation ( $n=12$ ;  $K_{1/2}$  value= $3.6 \times 10^{-6}$  M, Hill coefficient=1.0).



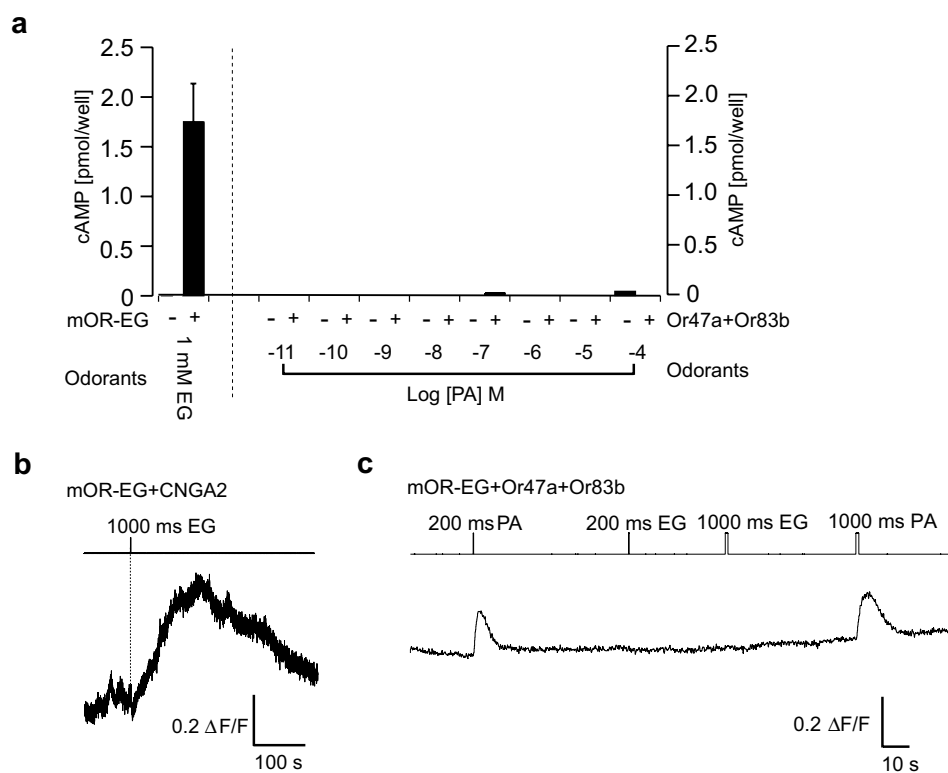
**Supplementary Figure S2I Spontaneous Ca<sup>2+</sup> influx in Or47a+Or83b-expressing HeLa cells.** **a**, Quantification of intracellular Ca<sup>2+</sup> concentrations in Or47a+Or83b expressing cells, with and without 10 mM EGTA applied extracellularly. Significance was assessed with ANOVA and *post hoc* test (\**p*<0.001; Or47a+Or83b *n*=29, pME18S *n*=56). Ca<sup>2+</sup> concentration was calibrated based on the maximal and minimal Fura-2 ratio and fluorescent intensity at 380 nm of individual cells treated with Ca<sup>2+</sup> ionophores **b**, Intracellular Ca<sup>2+</sup> level of Or47a+Or83b expressing cells measured with incubation in various Ringer's solutions with different Ca<sup>2+</sup> concentrations (*green*) and 10 mM EGTA solution (*white*). Solutions were applied during the time indicated by the *bars*. **c**, Bar plot of intracellular Ca<sup>2+</sup> levels at various extracellular Ca<sup>2+</sup> concentrations. The Fura-2 ratio was standardized to the magnitude of response to 100 μM PA in individual cells. Data are plotted as mean±s.e.m. (*n*=40).



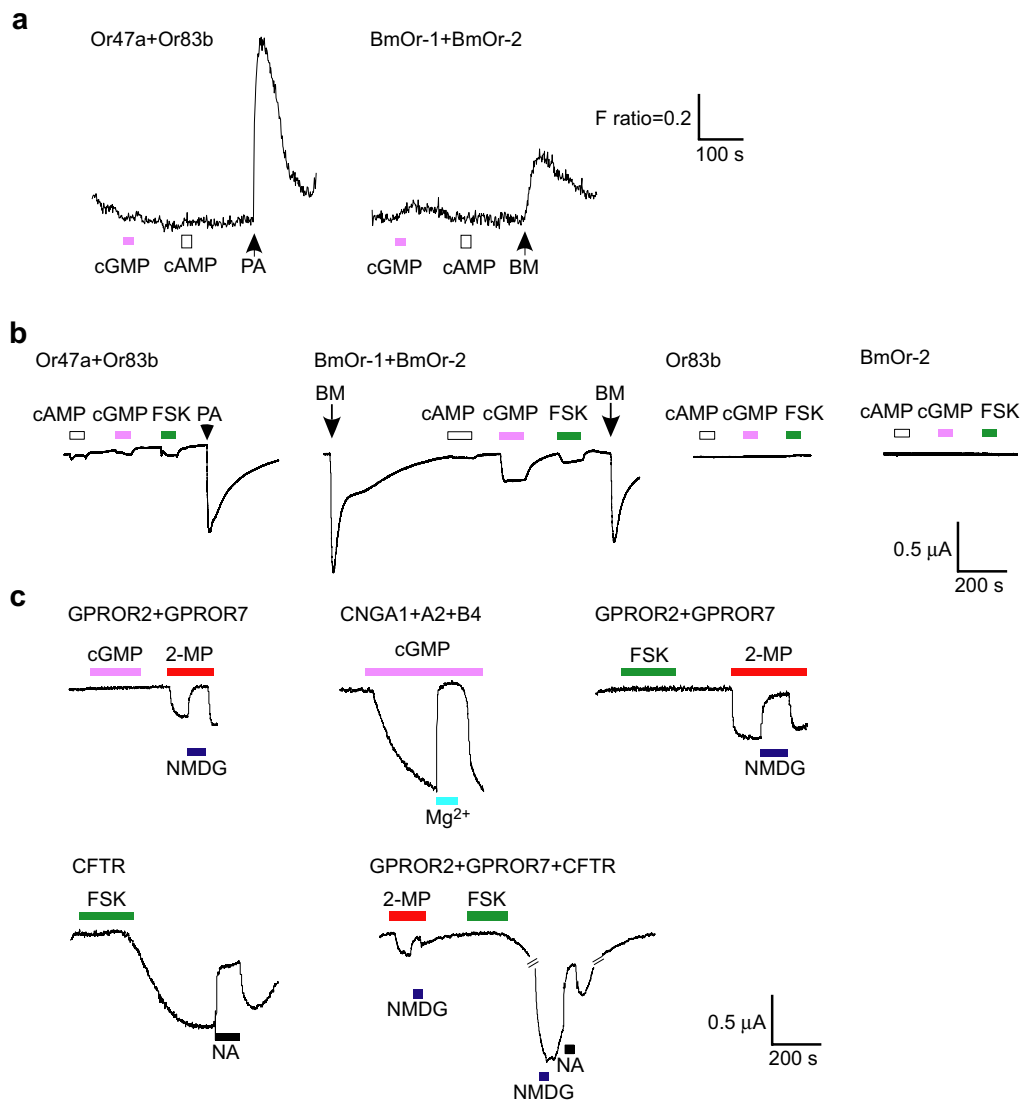
Supplementary Figure S3

**Supplementary Figure S3| Second messenger independent Or47a+Or83b currents.**

**a**, Current traces of Or47a+Or83b-expressing HeLa cells using a patch pipette containing the second messenger indicated at the *left*. *Top* bar indicates the timing of whole-cell configuration. *Arrowheads* indicate membrane capacitance to +1 mV voltage step pulse at 2 Hz. *Arrows* indicate stimulation with 100  $\mu$ M PA for 30 msec. Right traces were recorded 10 min after the achievement of whole-cell mode configuration. The slow activation of inward current of cGMP- and IP<sub>3</sub>- dialyzed cells is due to the activation of endogenous volume-sensitive outwardly rectifying anion channels (VSOR) which does not affect the transient odor-activated currents during the maximal activation of VSOR (>500 pA, data not shown). Holding potential was -60 mV. **b**, Outside-out patch clamp recording of a *Xenopus* oocyte membrane expressing Or47a+Or83b before stimulation (*left*) during 300  $\mu$ M PA stimulation (*middle*), and after wash out (*right*). Bottom traces of each panel indicate expansions of 300 ms current trace of single-channel recording at the positions indicated by numbers. The data in **b** were obtained from the same cell with voltage clamped at -80 mV. **c**, All-point current histograms of unitary events before (*blue*) and during application of the ligand PA (*red*) in the left and middle panel. Amplitude distributions were fitted with two Gaussian components (*black lines*). **d**, Outside-out patch clamp recording of an oocyte expressing Or47a+Or83b in the absence (*upper trace*) and presence (*lower trace*) of 300  $\mu$ M PA. The intracellular solution contained 1 mM GDP- $\beta$ -S. Voltage was clamped at -80 mV.



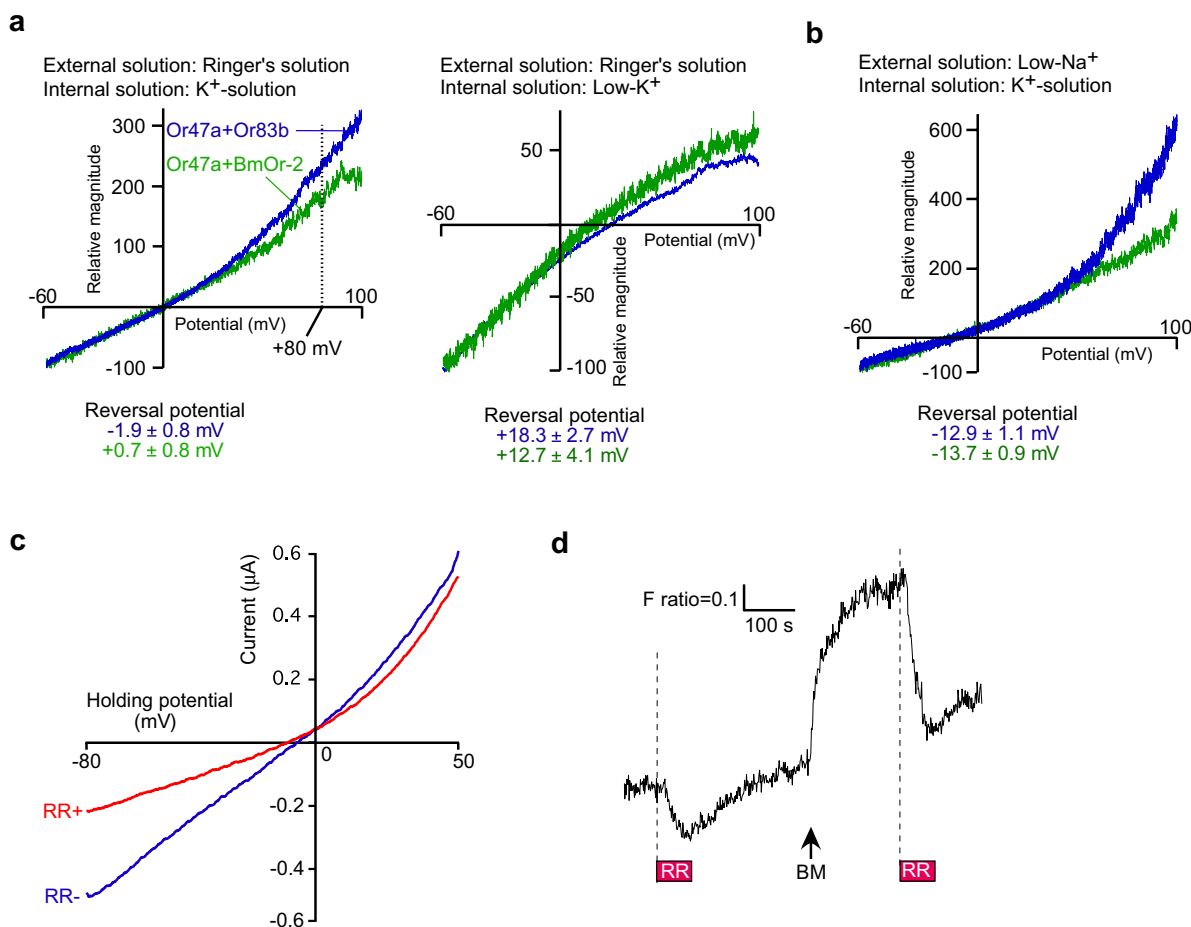
**Supplementary Figure S4| Examination of cAMP signaling in mOR-EG or Or47a+Or83b-expressing HEK293T cells. a**, Quantification of cAMP in HEK293T cells expressing mOR-EG or Or47a+Or83b. Various concentrations of PA ( $10^{-11}$  M to  $10^{-4}$  M) or EG (1 mM) were applied to Or47a+Or83b or mOR-EG-expressing cells, respectively. **b**, Calcium response to 1 mM EG in HEK293T cells expressing mOR-EG and mouse CNGA2. **c**, Calcium response profile of an HEK293T cell expressing Or47a+Or83b+mOR-EG to 100  $\mu$ M PA but not to 1 mM EG.



Supplementary Figure S5

**Supplementary Figure S5| Effect of cyclic nucleotides on insect OR activation**

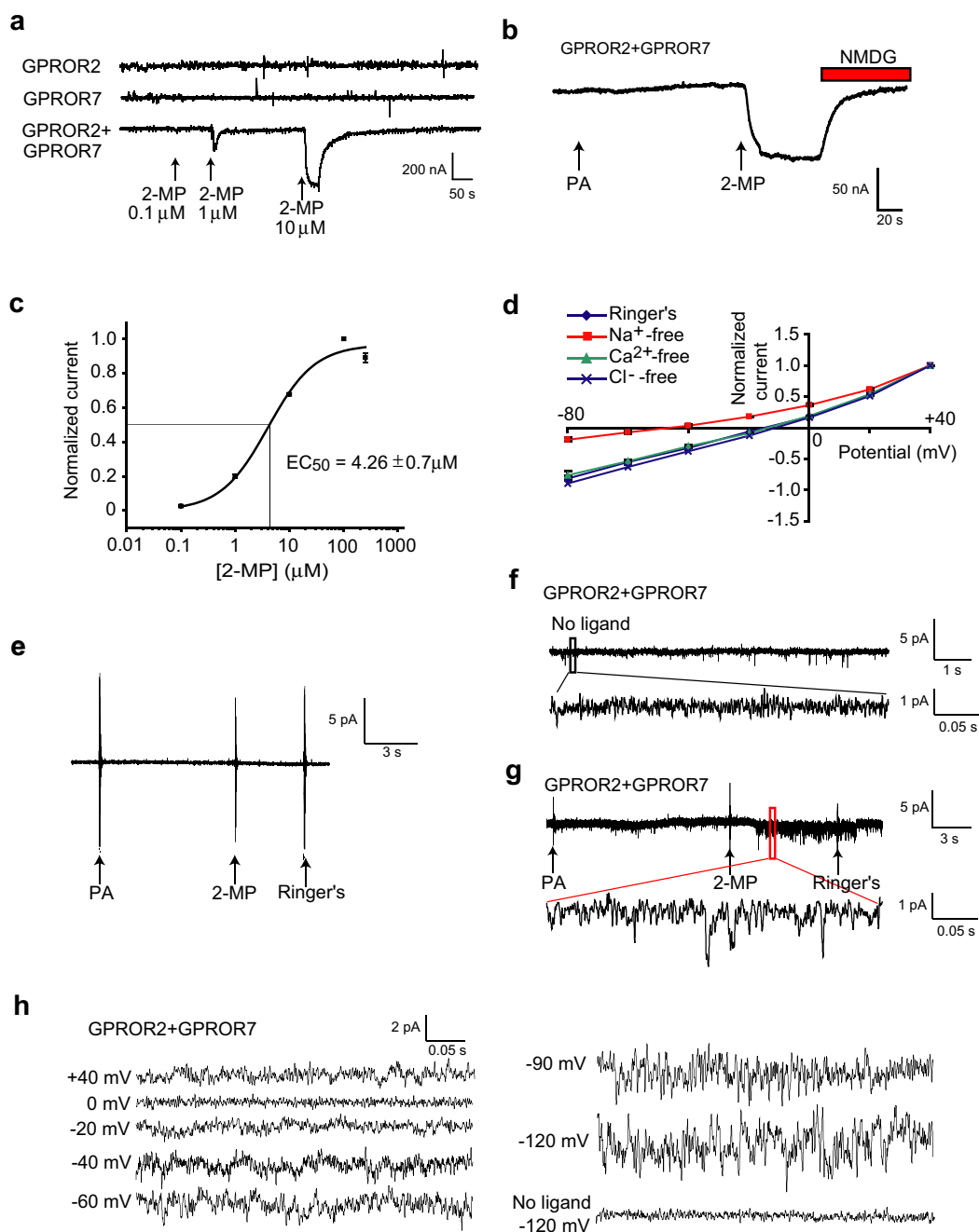
**a**,  $\text{Ca}^{2+}$  responses of HEK293T cells expressing Or47a+Or83b+ $\alpha_1$ -AR (left panel) or BmOr-1+ BmOr-2 (right panel) to a 10 sec application of 100  $\mu\text{M}$  PA and 100 nM NE or 10  $\mu\text{M}$  BM, respectively, and to 8-bromo-cAMP (500  $\mu\text{M}$ ) and 8-bromo-cGMP (500  $\mu\text{M}$ ). Neither 8-bromo-cGMP nor 8-bromo-cAMP produced  $\text{Ca}^{2+}$  responses in HEK293T cells expressing Or47a+Or83b. **b**, Current recording of oocytes expressing insect ORs (Or47a+Or83b, BmOr-1+BmOr-2, Or83b alone, or BmOr-2 alone). Small ligand-independent  $\text{Ca}^{2+}$  responses to 8-bromo-cGMP, 8-bromo-cAMP, and forskolin were seen in oocytes expressing BmOr-1+BmOr-2 or Or47a+Or83b, but not those expressing BmOr-2 or Or83b alone. However, these cyclic nucleotide-mediated responses were smaller than those evoked by ligand (cAMP:  $18 \pm 7.0\%$  and  $5.0 \pm 2.0\%$ , cGMP:  $15 \pm 3.0\%$  and  $3.2 \pm 0.75\%$ , Forskolin:  $3.6 \pm 0.8\%$  and  $5.8 \pm 1.7\%$ ; relative to bombykol and PA responses set to 100%, respectively). **c**, Current recording of oocytes expressing GPROR2+GPROR7, rat olfactory cyclic nucleotide-gated channels (CNGA1+CNGA2+CNGB4), and cystic fibrosis transmembrane conductance regulator (CFTR), as indicated at the top of each trace. The small, ligand-independent cyclic nucleotide effect was receptor-dependent, as oocytes expressing GPROR2+GPROR7 did not show any current responses upon stimulation with forskolin or 8-bromo-cGMP. To be sure that our cyclic nucleotide manipulations in oocytes were effective, we performed positive control experiments in oocytes expressing CNGA1+CNGA2+CNGB4 or CFTR, which showed a dramatic current response to 8-bromo-cGMP and forskolin, respectively. The currents were selective to the particular channel as the CNG current was inhibited by  $\text{Mg}^{2+}$  and the CFTR current was inhibited by a chloride-channel blocker, niflumic acid (NA). GPROR2+GPROR7-expressing oocytes showed a strong inward current response with application of the cognate ligand 2-MP, and this current was decreased by replacing  $\text{Na}^+$  in the bath with the non-permeant cation *N*-methyl-d-glucamine $^+$ , (NMDG $^+$ ), demonstrating that the inward current is largely carried by  $\text{Na}^+$  (see also Supplementary Fig. S8b). To ask whether activation of GPROR2+GPROR7 by 2-MP produced intracellular cAMP, we applied 2-MP to GPROR2+GPROR7 expressing oocytes that were also expressing CFTR, but found no characteristic evoked CFTR current. This suggests that odor stimulation of these mosquito receptors does not produce sufficient cAMP to gate CFTR. In **b** and **c**: Bombykol (BM, 10  $\mu\text{M}$ ) and PA (100  $\mu\text{M}$ ) were applied for 3 sec. 8-bromo-cAMP (cAMP, 100  $\mu\text{M}$ ), 8-bromo-cGMP (cGMP, 100  $\mu\text{M}$ ),  $\text{Mg}^{2+}$  (10 mM), and forskolin (FSK, 40  $\mu\text{M}$ ), 2-MP (10  $\mu\text{M}$ ), NMDG $^+$  (84.5 mM), and niflumic acid (NA, 1 mM) were applied during the time indicated by the bars above or below each trace.



### Supplementary Figure S6l Subunit-dependent functional properties of insect ORs.

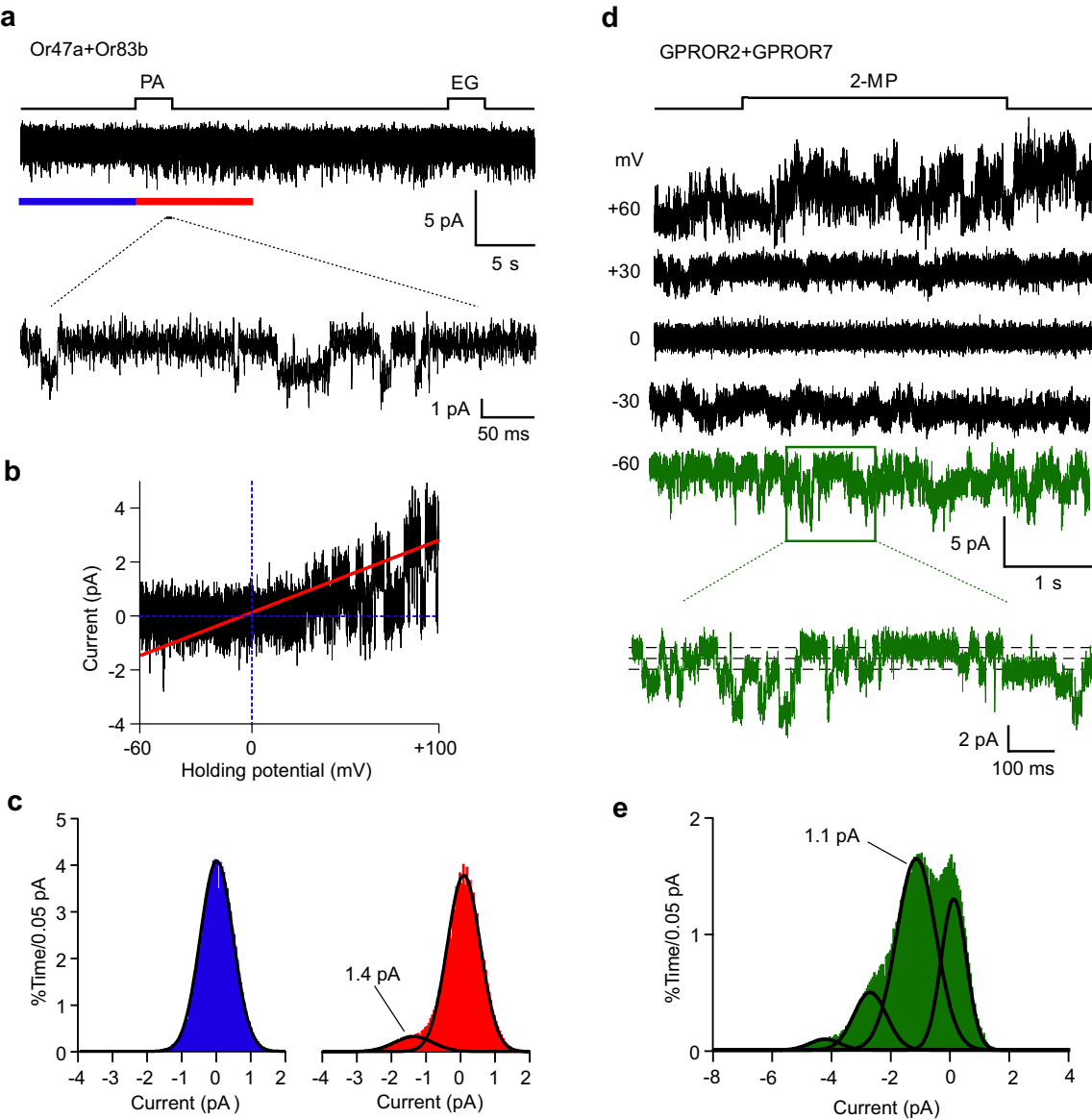
**a**, *Left panel* shows the I-V curve when normal Ringer's solution and K<sup>+</sup>-internal solution was perfused externally and internally, respectively (Or47a+Or83b: n=14; Or47a+BmOr-2: n=13). *Dotted line* indicates a holding potential at +80mV. *Right panel* was obtained when normal Ringer's solution and NMDG-internal solution were perfused extracellularly and intracellularly, respectively (Or47a+Or83b: n=11; Or47a+BmOr-2: n=13). **b**, NMDG-external solution and K<sup>+</sup>-internal solution was perfused extracellularly and intracellularly, respectively. The I-V curve was obtained by ramp voltage from -60 mV to +100 mV. The magnitudes of currents were standardized at a holding potential of -60 mV. The reversal potentials are indicated as mean±s.e.m (Or47a+Or83b: n=9; Or47a+BmOr-2: n=5). **c**, I-V curve of BM-induced current in oocytes expressing BmOr-1+BmOr-2 with or without ruthenium red (RR). The I-V curve was shifted to outward rectification in the presence of 50 μM RR. **d**, Ca<sup>2+</sup> responses of HEK293T cells expressing BmOr-1+BmOr-2 and effect of ruthenium red (RR). 10 μM BM was applied at the time indicated by *arrow* for 3 sec. Application of 50 μM RR is indicated by the *red bars*.





Supplementary Figure S7

**Supplementary Figure S7| Properties of GPROR2+GPROR7 currents measured in oocytes.** **a**, Dose-dependent macroscopic currents evoked by 2-MP require expression of both GPROR2 and GPROR7. **b**, GPROR2+GPROR7 current evoked by 2-MP is carried by  $\text{Na}^+$  ions because current was decreased when  $\text{Na}^+$  was substituted with impermeant NMDG<sup>+</sup> ions in the bath solution. **c**, Dose-response relationship of GPROR2+GPROR7 for 2-MP. The curve was fitted to the Hill equation ( $n=8$ ;  $K_{1/2}$  value =  $4.26 \pm 0.7 \mu\text{M}$ ; Hill coefficient =  $1.00 \pm 0.25$ ). **d**, I-V relationship defined for GPROR2+GPROR7. The I-V curve was obtained by step voltage from -80 mV to +40 mV (20 mV steps). The magnitude of currents was normalized at a holding potential of +40 mV ( $n=4$ ). Different curves represent I-V relationships under different ionic conditions: oocyte Ringer's solution (*blue diamond*);  $\text{Cl}^-$ -free solution (*blue cross*); and low- $\text{Na}^+$  solution (*red square*). The slope in the red curve represents a reduced conductance due to the reduced permeability of NMDG cations versus monovalent cations at negative potentials. At potentials higher than the reversal potential, we observed an outward current due to cations flowing from inside to outside of the cell. The other two I-V curves showed a reversal potential near the  $\text{Na}^+$  reversal potential, suggesting that the current was mainly carried by  $\text{Na}^+$  ions. **e**, Outside-out patch clamp recording of an uninjected oocyte clamped at -90 mV. Arrows indicate valve openings that delivered PA (300  $\mu\text{M}$ ), 2-MP (300  $\mu\text{M}$ ), or oocyte Ringer's solution. **f**, Outside-out patch clamp recording of an oocyte injected with GPROR2+GPROR7 in the absence of odor ligand. **g**, Outside-out patch clamp recording of a GPROR2+GPROR7-injected oocyte stimulated for 14 sec with 300  $\mu\text{M}$  of the non-agonist odor PA, followed by a 14 sec application of 300  $\mu\text{M}$  of the cognate agonist, 2-MP. Delay in current response to 2-MP is due to ~2 sec bath perfusion time lag. Oocyte Ringer's solution was perfused after the 14 sec 2-MP stimulation. The voltage was clamped at -90 mV. Bottom trace shows a time expansion during the 2-MP stimulation phase. **h**, Currents elicited in the same patch of a GPROR2+GPROR7-injected oocyte by 300  $\mu\text{M}$  2-MP at various holding potentials from +40 mV to -120 mV.



Supplementary Figure S8

**Supplementary Figure S8| Single-channel properties of Or47a+Or83b and GPROR2+GPROR7 in HEK293T cells.** **a**, Or47a+Or83b-expressing HEK293T membranes were stimulated for 3 sec with 300  $\mu$ M of the cognate agonist, PA, followed by a 3 sec application of 300  $\mu$ M of the non-agonist odor EG. The lower trace represents an expansion of the upper current trace of single-channel recording during PA stimulation. **b**, The I-V relationships of PA-activated single-channel events. The open-state currents at depolarizing potential were fitted with a linear function, which pass 1.4 pA at  $-60$  mV (*red*). Slope conductance was evaluated as 27 pS. Since the single channel conductance of odor-induced current was nearly 1 pA, we performed the ramp protocol to evaluate the slope conductance. **c**, The all-point current histogram was obtained from the region indicated by the *red bar* for PA stimulations in **a**. The histogram without stimulation was obtained from the region indicated by the *blue bar* in **a**. The amplitude distributions were fitted with a single Gaussian component (*black line*) without stimulation (left panel) and two Gaussians (*black line*) at PA stimulation (right panel). The mean peak current level (1.4 pA) was obtained from the fitted Gaussians. **d**, Multi-channels events of GPROR2+GPROR7 expressing HEK293T membranes with the stimulation of cognate agonist, 2-MP, for 3 sec at various holding potentials. The lower trace represents an expansion of the upper current trace of multi-channel recording during 2-MP stimulation at a holding potential of  $-60$  mV. **e**, The all-point current histogram was obtained from the current trace at a holding potential of  $-60$  mV (*green trace* in **d**). The amplitude distributions were fitted with four Gaussians (*black line*) at PA stimulation. The mean peak current level (1.1 pA) was obtained from the fitted Gaussians at  $-60$  mV, because 2-MP-induced currents were observed only when the holding potential was  $-60$  or  $+60$  mV. It is of note that we occasionally observed that eugenol at high concentrations inhibited the spontaneous activity of GPROR2+GPROR7 and Or47a+Or83b, but this was not found reliably.